



HAL
open science

Design and performance of wireless data gathering networks based on unicast random walk routing

Gwillerm Froc, Issam Mabrouki, Xavier Lagrange

► **To cite this version:**

Gwillerm Froc, Issam Mabrouki, Xavier Lagrange. Design and performance of wireless data gathering networks based on unicast random walk routing. *IEEE/ACM Transactions on Networking*, 2009, 17 (4), pp.1214-1227. 10.1109/TNET.2008.2006223 . hal-02141169

HAL Id: hal-02141169

<https://hal.science/hal-02141169>

Submitted on 30 Mar 2022

HAL is a multi-disciplinary open access archive for the deposit and dissemination of scientific research documents, whether they are published or not. The documents may come from teaching and research institutions in France or abroad, or from public or private research centers.

L'archive ouverte pluridisciplinaire **HAL**, est destinée au dépôt et à la diffusion de documents scientifiques de niveau recherche, publiés ou non, émanant des établissements d'enseignement et de recherche français ou étrangers, des laboratoires publics ou privés.



Distributed under a Creative Commons Attribution - NonCommercial 4.0 International License

Design and Performance of Wireless Data Gathering Networks Based on Unicast Random Walk Routing

Gwillerm Froc, Issam Mabrouki, and Xavier Lagrange

Abstract—Wireless environment monitoring applications with significantly relaxed quality-of-service constraints are emerging. Hence, the possibility to use rough low knowledge routing in sensor networks to reduce hardware resource and software complexity is questionable. Moreover, low knowledge handling allows better genericity, which is of interest, for instance, for basic operation enabling system set-up. In this framework, this paper revisits stateless unicast random walk routing in wireless sensor networks. Based on random walk theory, original closed-form expressions of the delay, the power consumption and related spatial behaviors are provided according to the scale of the system. Basic properties of such a random routing are discussed. Exploiting its properties, data gathering schemes that fulfill the requirements of the application with rather good energy efficiency are then identified.

Index Terms—Data gathering, quality of service (QoS), random walk, routing, wireless sensor networks.

I. INTRODUCTION

OVER the last decade, research into wireless sensor networks has been burgeoning leading to first developments and products that are about to deeply modify the way society interacts with the physical world. This research relies on continued technological progress in small, cheap and low power consuming sensors, actuators, radio front-ends and processors. It enables a wide range of applications including disaster relief, intelligent buildings, logistics, safety and industrial and environment monitoring as overviewed in [1].

However, not all of the wireless sensor applications have the same requirements and QoS constraints. Yet, referring to [3]–[5] for example, it is worth noting that many environment monitoring applications work under infrequent updates of a few minutes or longer and can tolerate data gathering delay of one second up to a few tens of seconds, or can withstand temporary gaps in the collected data set like in the farm’s soil moisture wireless sensor system depicted in [5]. Thus, for such Wireless Data Gathering Networks (WDGN), constraints on latency and collected data quality can be significantly relaxed. Nevertheless, the implications of these relaxed constraints have not been examined specifically in the literature although this should allow room for rough but low complex solutions.

Dealing with routing, stateless mechanisms are “rough but low complex” and thus may be helpful for low cost WDCN. Furthermore, they are generic which is also of interest in a transient way for state-based routing when the topology is unknown. For instance, it may be useful when networks have dynamic devices that need to be frequently updated or when the network is often extended [6].

Therefore, in the context of relaxed QoS constraints, this paper revisits random walk options for routing by evaluating unicast random walk routing schemes. To model the system, known results from the random walk theory are applied on a square lattice. This latter includes traps to account for the presence of the collectors. Original analytical closed-form expressions, valid whatever the scale is, are derived for delays, spatial properties and energy consumption. It is then possible to study performance issues and basic properties according to the *sensor – collector* density ratio which scales the random walk. We find that load balancing is achieved, the mean delay can be acceptable with not-so-large scale and meet the system requirements when WDCN are considered. Moreover, suitable data gathering schemes are deduced at system level. It is shown that these schemes can be energy-efficient.

The rest of this paper is organized as follows. Section II draws up main features of WDCN and justifies the use of unicast random walk routing. In Section III we present the model to describe unicast random walk routing. Then in Section IV, the performance statistics are derived. Results are discussed in Section V and suitable data gathering schemes are proposed at system level. Lastly, the conclusion sums up the results and points out how fruitful could be the framework this paper defines.

II. UNICAST RANDOM WALK ROUTING FOR WIRELESS DATA GATHERING NETWORKS AND RELATED WORK

Here, the features of WDCN are introduced. It is shown how the related requirements suggest the use of multihop unicast routing to convey the data. The pertinence of random schemes to choose the next relay node at each hop is also discussed.

The WDCN considered are made up of sensors and collectors. There are typically between 10 to 1000 sensors from which information is collected within between 1 and a few 10s of seconds for every gathering cycle. The data size is about 1–10 bytes. The gathering cycles occur from time to time with a period of a few 10s of minutes. The monitoring can tolerate temporary gaps in the gathered data set. The collectors act as sinks. They can have more computing resource than sensors and can communicate with the remote application. Since they are more complex and costly, their number has to be low.

Under these assumptions, we want to identify transport schemes that would allow (i) a low system cost and (ii) a

G. Froc and I. Mabrouki are with Mitsubishi-Electric R&D Centre Europe, 35 708 Rennes, France (e-mail: froc@tcl.ite.mee.com; mabrouki@tcl.ite.mee.com).

X. Lagrange is with Institut TELECOM, TELECOM Bretagne, 35576 Cesson Sévigné France (e-mail: xavier.lagrange@telecom-bretagne.eu).

system lifetime as long as possible. The low cost constraint (i) implies that hardware and software resources to implement protocols should be reduced as far as possible. At first, the lifetime constraint (ii) is satisfied by scaling down the activation of the system to the gathering cycles. At the hardware level, this requires only a clock and a timer. Now, regarding the gathering cycles, to convey the data from a source to a destination, analyses show that, in an homogeneous system, the multihop strategy is better since the communication energy consumption dominates the energy consumption induced by the circuitry [7]–[9]. This means envisaging strategies with relaying capable sensors. So, jointly considering (i) and (ii) infers that the routing has to be based on an energy efficient low complex multihop scheme. Now, to be consistent with the energy consumption minimization, we do not allow multiple copies of a message. This leads to unicast multihop routing.

Here two issues arise. First, energy minimization of the routing and low complexity are quite antinomic. Indeed, the minimization energy problem applies to a large state space that accounts for time evolving parameters such as propagation or data rates [9]. Hence, to solve it, decisions must be taken from a large amount of shared information. This requires a great deal of hardware, software and updating signalling exchanges which induces an energy overhead and is contrary to the low complexity requirement (ii). In addition, it has been underlined that the energy depletion should be distributed over the set of sensors to avoid the burning node effects and to ensure uniform QoS over time and space [10]–[12]. This argues for non-deterministic and more specifically random walk approaches for routing. Indeed, the use of random walk approaches is common to reduce complexity in large scale systems because it enables stateless operations. It has already been suggested for routing in wireless systems. In [13] constrained random walk multipath routing is proposed to allow load balancing in wireless sensor networks where nodes switch between active and inactive states at random times to save energy. More efficient than flooding, gossiping techniques to spread information in possibly unconnected networks [14], [15] are also related to random walk approaches since, at each hop, messages are forwarded to their neighbors with a certain probability. However, the results presented are strongly dependent on the connectivity of the system and they have to be analyzed in light of percolation theory [16] first. Moreover, the generation of multiple copies of a given message to propagate the information is allowed. However, our study is focused on the randomness of the routing scheme assuming that the network is connected and allows only one copy of a given message to circulate. Rumor routing [17] aims at building a path between query and related event by flooding both event and query information up to a certain extent. Then, the generated agents are unicasted until they link both domains or die. When the agent forwarding policy follows a random scheme, rumor routing is a kind of unicast random walk routing where the cross section of the event-query intersection (a path between source and destination) is enhanced by the event and query flooding extension. However, results are discussed based on simulations that do not account for strict random agent forwarding scheme. Therefore, specific insights into unicast random walk routing cannot be revealed. It may be that often, the performance of random walk approaches are considered as

too poor [1]. Note that in the relaxed constraints context this paper addresses, we specifically want to exploit the fact that lower performance are acceptable. Moreover, recently Zhong [18] pointed out how effective random walk schemes could be in dynamic and decentralized settings.

III. RANDOM WALK MODELLING

This section presents the model used to study unicast random walk routing (URWR). The network is represented by an infinite square lattice. The transmission of messages is allowed only between nearest neighbors. URWR then corresponds to a random walk over an infinite square lattice for which basic statistics have already been derived [20]. So here, we just recall the formalism and general expressions of basic statistics for both homogenous systems and systems perturbed by a central data gathering scheme which allows us to account for the presence of collectors.

A. Random Walk Parameters Definition

Let us consider a graph $\mathcal{G}(\Omega, E)$ where Ω is a countable set of nodes wirelessly connected pairwise by a set E of undirected edges to represent communication links between nodes. Every node can be the source or the destination of a message, as well as a relay for communications between any other pair of nodes. A message called *random walker* is randomly forwarded from relay node to relay node until it reaches its destination. We assume that time is slotted and that a 1-hop transmission consumes 1 time slot.

To describe the random walk, the *transition function* of the random walk is introduced. It defines at a given node \vec{r} the probability $p(\vec{r}, \vec{s})$ to reach node \vec{s} . As a probability, it is a non-negative real and verifies $\sum_{\vec{s} \in \Omega} p(\vec{r}, \vec{s}) = 1$.

Let $P_n(\vec{r}, \vec{s})$ be the probability for the packet to be at node \vec{s} after n hops, given that it has been issued at node \vec{r} . It is called the *node occupation probability*. Let $F_n(\vec{r}, \vec{s})$ be the probability for the packet to arrive at node \vec{s} for the *first* time on the n th hop, given that the walk started at node \vec{r} . It is referred as the *first-passage probability*. These probabilities are key parameters from which main results can be deduced. They are defined for $n \geq 1$. For $n = 0$, they are set down to

$$P_0(\vec{r}, \vec{s}) = \delta_{\vec{r}\vec{s}} \quad \text{and} \quad F_0(\vec{r}, \vec{s}) = 0. \quad (1)$$

Then, it is useful to introduce the generating function formalism [21] that capture probabilities for all defined n

$$g(\vec{r}, \vec{s} | \xi) = \sum_{n \geq 0} g_n(\vec{r}, \vec{s}) \xi^n, \quad (2)$$

ξ being a complex variable small enough to ensure the convergence of the series. Basic statistics such as the expectation and the variance can be derived from g .

Let then $P(\vec{r}, \vec{s} | \xi)$ and $F(\vec{r}, \vec{s} | \xi)$ be respectively the generating function of the node occupation probability and of the first-passage probability. At fixed \vec{r} , $P(\vec{r}, \vec{s} | \xi)$ satisfies the normalization condition

$$\sum_{\vec{s} \in \Omega} P(\vec{r}, \vec{s} | \xi) = \frac{1}{1 - \xi}. \quad (3)$$

Illustrating the law of total probability, $P(\vec{r}, \vec{s} | \xi)$ and $F(\vec{r}, \vec{s} | \xi)$ are related to each other according to the relation

$$P(\vec{r}, \vec{s} | \xi) = \delta_{\vec{r}\vec{s}} + F(\vec{r}, \vec{s} | \xi) P(\vec{s}, \vec{s} | \xi), \quad \vec{r}, \vec{s} \in \Omega. \quad (4)$$

Now, how likely does the walk evolve in the future under some initial conditions? It is possible to describe the walk through a set of equations called the *evolution laws*, governing the walk evolution. Indeed, $P(\vec{r}, \vec{s} | \xi)$, which completely determines the node occupation probability distribution over the nodes of Ω at fixed n , can be described as the solution of two equivalent evolution laws superficially different but mathematically equivalent because of the constancy with time of the transition probabilities and our ability to identify first and last hops in an n -hop walk

$$P(\vec{r}, \vec{s} | \xi) = \delta_{\vec{r}\vec{s}} + \xi \sum_{\vec{s}' \in \Omega} P(\vec{r}, \vec{s}' | \xi) p(\vec{s}', \vec{s}) \quad (5)$$

$$P(\vec{r}, \vec{s} | \xi) = \delta_{\vec{r}\vec{s}} + \xi \sum_{\vec{s}' \in \Omega} p(\vec{r}, \vec{s}') P(\vec{s}', \vec{s} | \xi). \quad (6)$$

Now, let us introduce the discrete linear *transition operator* \mathcal{T} that is acting on an unknown function $u(\vec{s})$ as

$$(\mathcal{T}u)(\vec{s}) = u(\vec{s}) - \xi \sum_{\vec{s}' \in \Omega} u(\vec{s}') p(\vec{s}', \vec{s}), \quad (7)$$

Then, if we define a s -dependent source term $f(\vec{s})$, the evolution law (5) can be identified to the nonhomogeneous discrete linear differential equation

$$(\mathcal{T}u)(\vec{s}) = f(\vec{s}), \quad (8)$$

in the special case $f(\vec{s}) = \delta_{\vec{r}\vec{s}}$, where \vec{s} is the variable and \vec{r} is a parameter. $P(\vec{r}, \vec{s} | \xi)$ is then just the *Green function* of (8).

Since the general solution of a nonhomogeneous discrete linear differential equation can be constructed by the convolution of its Green function with the source term

$$u(\vec{s}) = \sum_{\vec{r} \in \Omega} f(\vec{r}) P(\vec{r}, \vec{s} | \xi), \quad (9)$$

it can be deduced that it is still possible to derive solutions for s -dependent random walk potentials from basic one related to $P(\vec{r}, \vec{s} | \xi)$. This arises especially for nonhomogeneous random walks whose transition functions are resulting from added perturbation terms to spatial homogeneous transition functions. Below, we exploit this technique to derive from the homogeneous random walk, the case of a central data gathering scheme where all sensor nodes send their data to collector nodes that behave as trapping sites.

B. Homogeneous Random Walk on a Lattice

In the previous paragraph, no hypothesis, neither on the structure of state space Ω nor on transition function $p(\vec{r}, \vec{s})$, has been assumed while establishing evolution laws (5) and (6). In this section, the random walk problem is specified further by translating WDGn requirements into mathematical constraints. Some restrictions are introduced to ease the derivation of the closed-form solution of the evolution laws.

As a starting point, it is assumed that all nodes are of same nature and behave similarly in an homogeneous environment.

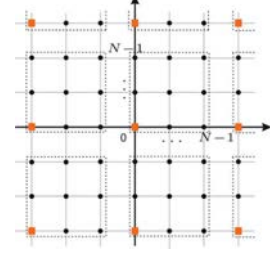


Fig. 1. $N \times N$ regular square sensor lattice. Collectors are introduced at the origin of the elementary cells in the case of central data gathering scheme.

Every node acts simultaneously as source, destination as well as relay for the other ones. Next, it is considered that the random walk takes place on an infinite regular structure made up of the repetition of an elementary cell being a finite square lattices \mathcal{L} of size $N \times N$ as presented in Fig. 1. Moreover, only equally probable nearest neighbor transitions are allowed. Such assumptions are of threefold interest. First, the regularity of the structure can fit the averaged characteristics of WDGn (e.g., mesh or grid networks). Second, the model is simple enough to allow an analytical study of the random walk problem while still being useful to incorporate the specific key issues of wireless sensor networks such as the data forwarding policy. Third, more complex situation can be considered as a perturbation of this basic scheme. This is the case when collector nodes are present, which will be studied bellow.

The transition function $p(\vec{r}, \vec{s})$ is then

$$p(\vec{r}, \vec{s}) = \frac{1}{4} [\delta_{\vec{s}, \vec{r} + \vec{e}_1} + \delta_{\vec{s}, \vec{r} - \vec{e}_1} + \delta_{\vec{s}, \vec{r} + \vec{e}_2} + \delta_{\vec{s}, \vec{r} - \vec{e}_2}] \quad (10)$$

where \vec{e}_1 and \vec{e}_2 denote the unit vectors of the orthonormal reference. $\vec{r} \pm \vec{e}_i$ is interpreted modulo N . Spatial homogeneity has been assumed. It means that the data forwarding model depends only on the relative position of the nodes. Hence it translates in transition function $p(\vec{r}, \vec{s})$ that verifies

$$p(\vec{r}, \vec{s}) = p(\mathbf{0}, \vec{s} - \vec{r}) \quad \text{for all } \vec{r}, \vec{s} \in \mathcal{L} \quad (11)$$

where $\vec{s} - \vec{r}$ is interpreted modulo N , i.e., periodically. So, it can be deduced that the node occupation probability generating function $P(\vec{r}, \vec{s} | \xi)$ also verifies the spatial homogeneity property, and is then really determined by the single-point function $P(\mathbf{0}, \vec{s} | \xi)$ on which the following developments are based.

In other respects, since there is no directional bias on any hop,

$$P(\vec{r}, \vec{s} | \xi) = P(\vec{s}, \vec{r} | \xi) \quad \text{for all } \vec{r}, \vec{s} \in \mathcal{L}, \quad (12)$$

and the considered random walk is deemed *symmetric*.

The regular structure of the random walk allows to define discrete Fourier transforms and ensures that $P(\mathbf{0}, \vec{s} | \xi)$ can be explicitly derived. The detail calculation can be found in [20]. To sum up, the first step is to define the Fourier series $\lambda(\vec{\theta})$ and $\hat{P}_n(\mathbf{0}, \vec{\theta})$ associated with the transition probabilities $p(\mathbf{0}, \vec{s})$ and the site occupation probability $P_n(\mathbf{0}, \vec{s})$ respectively. Then, taking the Fourier series of both sides of (5), one finds that $\hat{P}_n(\mathbf{0}, \vec{\theta}) = \lambda(\vec{\theta})^n$. Inverting back $\hat{P}_n(\mathbf{0}, \vec{\theta})$, one has

$$P_n(\mathbf{0}, \vec{s}) = \frac{1}{(2\pi)^2} \int_{\vec{\theta} \in [-\pi, \pi]^2} \lambda(\vec{\theta})^n e^{-i\vec{s}\vec{\theta}} d^2\vec{\theta}. \quad (13)$$

Multiplying both sides of (13) by ξ^n , summing over n , inverting the integration and summation orders, and summing the resulting geometric series in the integrand, we have

$$P(\mathbf{0}, \vec{s} | \xi) = \frac{1}{(2\pi)^2} \int_{\vec{\theta} \in [-\pi, \pi]^2} \frac{e^{-i\vec{s}\cdot\vec{\theta}}}{1 - \xi\lambda(\vec{\theta})} d^2\vec{\theta}. \quad (14)$$

Then, substituting in (14) the expression of the Fourier Series $\lambda(\vec{\theta})$ of $p(\mathbf{0}, \vec{s})$ that is given by (10), one obtains

$$P(\mathbf{0}, \vec{s} | \xi) = \frac{1}{N^2} \sum_{m_1, m_2=0}^{N-1} \frac{e^{-i\frac{2\pi}{N}[m_1 s_1 + m_2 s_2]}}{1 - \frac{\xi}{2} [\cos(\frac{2\pi}{N} m_1) + \cos(\frac{2\pi}{N} m_2)]}. \quad (15)$$

C. Central Data Gathering Scheme

To model data gathering schemes that distinguish between sensors and collectors, a sink node located at the origin is introduced. A packet arriving at the sink node never leaves. However, by introducing two types of nodes, lattice nodes are no longer equivalent and the spatial homogeneity assumed in case of the homogeneous walk is broken down. To solve the problem in this non-homogeneous case, we make use of the perturbation method considering that the random walk problem associated with the central data gathering scheme is resulting from adding perturbations to the one associated with the homogeneous walk, for which an explicit solution of the node occupation probability generating function has been provided in (15). Then, from (9) a solution can be deduced.

Let $p^\dagger(\vec{r}, \vec{s})$ and $q(\vec{r}, \vec{s})$ denote the transition functions associated with the central data gathering scheme and the perturbation term respectively. The perturbation term is produced from adding the sink node, recalling that a packet arriving to the sink node never leaves. As $p(\vec{r}, \vec{s})$ is the transition function of the homogeneous walk, one has

$$p^\dagger(\vec{r}, \vec{s}) = p(\vec{r}, \vec{s}) + q(\vec{r}, \vec{s}) \quad (16)$$

with

$$q(\vec{r}, \vec{s}) = \begin{cases} 0 & \text{if } \vec{r} \neq \mathbf{0} \\ \delta_{\vec{r}\vec{s}} - p(\vec{r}, \vec{s}) & \text{else} \end{cases} \quad (17)$$

and

$$p^\dagger(\vec{r}, \vec{s}) = \begin{cases} p(\vec{r}, \vec{s}) & \text{if } \vec{r} \neq \mathbf{0} \\ \delta_{\vec{r}\vec{s}} & \text{else.} \end{cases} \quad (18)$$

Now, the node occupation probability generating function associated to the central data gathering scheme denoted by $P^\dagger(\vec{r}, \vec{s} | \xi)$ has to be evaluated.

Theorem 3.1: $P^\dagger(\vec{r}, \vec{s} | \xi)$ can be expressed in function of $P(\vec{r}, \vec{s} | \xi)$, as follows:

$$P^\dagger(\vec{r}, \vec{s} | \xi) = P(\vec{r}, \vec{s} | \xi) + (1 - \xi)^{-1} \frac{P(\vec{r}, \mathbf{0} | \xi)}{P(\mathbf{0}, \mathbf{0} | \xi)} \delta_{\mathbf{0}\vec{s}} - P(\mathbf{0}, \vec{s} | \xi) \frac{P(\vec{r}, \mathbf{0} | \xi)}{P(\mathbf{0}, \mathbf{0} | \xi)} \quad (19)$$

Proof: This proof is based on the resolution of the evolution law verified by $P^\dagger(\vec{r}, \vec{s} | \xi)$, through the aid of (9). Indeed, from (5), $P^\dagger(\vec{r}, \vec{s} | \xi)$ satisfies

$$P^\dagger(\vec{r}, \vec{s} | \xi) = \delta_{\vec{r}\vec{s}} + \xi \sum_{\vec{s}' \in \mathcal{L}} P^\dagger(\vec{r}, \vec{s}' | \xi) p^\dagger(\vec{s}', \vec{s}). \quad (20)$$

Plugging (16) into (20) and substituting the expression of the perturbation term embodied in (17), we find

$$P^\dagger(\vec{r}, \vec{s} | \xi) - \xi \sum_{\vec{s}' \in \mathcal{L}} P^\dagger(\vec{r}, \vec{s}' | \xi) p(\vec{s}', \vec{s}) = \delta_{\vec{r}\vec{s}} + \xi P^\dagger(\vec{r}, \mathbf{0} | \xi) (\delta_{\mathbf{0}\vec{s}} - p(\mathbf{0}, \vec{s})). \quad (21)$$

The left-hand side of (21) can be recognized as the transition operator \mathfrak{T} acting on $P^\dagger(\vec{r}, \vec{s} | \xi)$. Therefore, referring to (9), $P^\dagger(\vec{r}, \vec{s} | \xi)$ can be expressed as the convolution of Green function $P(\vec{r}, \vec{s} | \xi)$ with the right-side of (21). We obtain

$$P^\dagger(\vec{r}, \vec{s} | \xi) = P(\vec{r}, \vec{s} | \xi) + P^\dagger(\vec{r}, \mathbf{0} | \xi) \times \xi \left(P^\dagger(\mathbf{0}, \vec{s} | \xi) - \sum_{\vec{s}' \in \mathcal{L}} p(\mathbf{0}, \vec{s}') P(\vec{s}', \vec{s} | \xi) \right). \quad (22)$$

Using (6), we can eliminate the sum in (22) and get

$$P^\dagger(\vec{r}, \vec{s} | \xi) = P(\vec{r}, \vec{s} | \xi) + P^\dagger(\vec{r}, \mathbf{0} | \xi) \delta_{\mathbf{0}\vec{s}} - (1 - \xi) P^\dagger(\vec{r}, \mathbf{0} | \xi) P(\mathbf{0}, \vec{s} | \xi). \quad (23)$$

This relation enables us to infer the value of $P^\dagger(\vec{r}, \vec{s} | \xi)$ in function of $P(\vec{r}, \vec{s} | \xi)$ once we know $P^\dagger(\vec{r}, \mathbf{0} | \xi)$. By setting $\vec{s} = \mathbf{0}$ in (23), it follows that

$$P^\dagger(\vec{r}, \mathbf{0} | \xi) = (1 - \xi)^{-1} \frac{P(\vec{r}, \mathbf{0} | \xi)}{P(\mathbf{0}, \mathbf{0} | \xi)}. \quad (24)$$

Using this expression of $P^\dagger(\vec{r}, \mathbf{0} | \xi)$ in (23) leads to (19). ■

IV. UNICAST RANDOM WALK ROUTING PERFORMANCE

The objective of this section is to evaluate the performance of Unicast Random Walk Routing (URWR). Beyond basic random walk results presented above, we specifically derive original closed-form expressions that apply even for small scale systems. First, to exhibit in a synthetic way the general system behavior, we define and look at data gathering delays averaged over the network considering all sensors as equivalent. Next, the spatial dependency of the data gathering delay is scrutinized. Then, the impact of URWR on energy consumption is studied. The results are discussed and from the properties of the random walk on such system, data gathering schemes that reduce the energy consumption are proposed.

A. Data Gathering Delay Averaged Over the Network

The data gathering delay is the time or the number of hops it takes for a message issued from an arbitrary sensor node $\vec{s} = \{s_1, s_2\}$ to reach the sink node for the first time where it is trapped. We denote $\mathcal{D}_N^\dagger(\vec{s})$ this random variable. Let $E(\mathcal{D}_N^\dagger)$ be the mean of $\mathcal{D}_N^\dagger(\vec{s})$ over the entire set of sensors. We call it *System Data Gathering Delay* in the following. Here, it is looked at the *mean*, or in mathematical parlance, the expectation, and the *variance* of \mathcal{D}_N^\dagger . The equivalence of the sensor nodes is ensured assuming a uniform traffic generation distribution, that is, a packet has the same probability of being generated at any sensor node, with probability $\frac{1}{N^2-1}$.

First, the generating function is determined. Then, expressions of the expectation and the variance of \mathcal{D}_N^\dagger are exhibited. It is shown that they are relevant even for small system sizes.

1) *Generating Function:* Let $G_n^\dagger(N)$ be the probability that a packet initially issued at any sensor node will be trapped at the sink node on the n th hop

$$G_n^\dagger(N) = Pr\{\mathcal{D}_N^\dagger = n\}, \quad n \geq 0.$$

Now, we express $G^\dagger(N|\xi)$ in function of $P(\mathbf{0}, \mathbf{0}|\xi)$.

As a starting point, let $F_n^\dagger(\vec{\mathbf{r}}, \mathbf{0})$ and $F^\dagger(\vec{\mathbf{r}}, \mathbf{0}|\xi)$ be respectively the first passage probability of arriving at the sink node on the n th hop, given that the packet has been issued at sensor node $\vec{\mathbf{r}}$, and its generating function. Using the law of total probability, it is possible to decompose the event that a packet will be trapped at the sink node on the n th hop, which has the probability $G_n^\dagger(N)$, into the $N^2 - 1$ mutually exclusive events that the packet is initially generated at sensor node $\vec{\mathbf{r}}$ with probability $\frac{1}{N^2-1}$, and then arrives at the sink node for the *first* time after n hops, which has the probability $F_n^\dagger(\vec{\mathbf{r}}, \mathbf{0})$. It comes

$$G_n^\dagger(N) = \frac{1}{N^2-1} \sum_{\vec{\mathbf{r}} \neq \mathbf{0}} F_n^\dagger(\vec{\mathbf{r}}, \mathbf{0}), \quad n \geq 0.$$

Multiplying both sides by ξ^n and summing over n , we obtain

$$G^\dagger(N|\xi) = \frac{1}{N^2-1} \sum_{\vec{\mathbf{r}} \neq \mathbf{0}} F^\dagger(\vec{\mathbf{r}}, \mathbf{0}|\xi). \quad (25)$$

Then using (4) that translates the law of total probability and links $F^\dagger(\vec{\mathbf{r}}, \mathbf{0}|\xi)$ to $P^\dagger(\vec{\mathbf{r}}, \mathbf{0}|\xi)$, next, applying Theorem 3.1 that relates $P^\dagger(\vec{\mathbf{r}}, \mathbf{0}|\xi)$ to $P(\vec{\mathbf{r}}, \mathbf{0}|\xi)$, one finds

$$F^\dagger(\vec{\mathbf{r}}, \mathbf{0}|\xi) = \frac{P(\vec{\mathbf{r}}, \mathbf{0}|\xi)}{P(\vec{\mathbf{0}}, \mathbf{0}|\xi)} \quad (26)$$

and (25) becomes

$$G^\dagger(N|\xi) = \frac{1}{(N^2-1)P(\mathbf{0}, \mathbf{0}|\xi)} \left[\sum_{\vec{\mathbf{r}} \in \mathcal{L}} P(\vec{\mathbf{r}}, \mathbf{0}|\xi) - P(\mathbf{0}, \mathbf{0}|\xi) \right]. \quad (27)$$

Using successively the symmetric property (12) of the node occupation probability generating function associated with the homogeneous walk and the normalization condition (3), the sum embodied in (27) can be simplified as follows:

$$\sum_{\vec{\mathbf{r}} \in \mathcal{L}} P(\vec{\mathbf{r}}, \mathbf{0}|\xi) = \sum_{\vec{\mathbf{r}} \in \mathcal{L}} P(\mathbf{0}, \vec{\mathbf{r}}|\xi) = \frac{1}{1-\xi}. \quad (28)$$

Plugging (28) into (27), we obtain

$$G^\dagger(N|\xi) = \frac{1}{N^2-1} \left\{ \frac{1}{(1-\xi)P(\mathbf{0}, \mathbf{0}|\xi)} - 1 \right\}. \quad (29)$$

2) Mean of System Data Gathering Delay:

Result 4.1: The mean or expectation of System Data Gathering Delay has the following closed-form expression

$$E(\mathcal{D}_N^\dagger) = \frac{1}{3}N^2 + \frac{N^4}{N^2-1} \varphi_N(\mathbf{0}, 1) \quad (30)$$

where $\varphi_N(\vec{\mathbf{s}}, \xi)$ is an N -dependent holomorphic function defined by (59) in Appendix A.

Proof: The mean of System Data Gathering Delay is

$$E(\mathcal{D}_N^\dagger) = \sum_{n=0}^{\infty} nG_n^\dagger(N) = \lim_{\xi \rightarrow 1^-} \frac{\partial}{\partial \xi} G^\dagger(N|\xi). \quad (31)$$

Substituting in (31) the expression of $G^\dagger(N|\xi)$ given by (29), would not lead directly to an explicit expression for $E(\mathcal{D}_N^\dagger)$. So, instead, we extract a closed form considering the Taylor series expansion of $G^\dagger(N|\xi)$ as $\xi \rightarrow 1^-$. Indeed, (62) in Appendix A provides an asymptotic expansion of $P(\mathbf{0}, \vec{\mathbf{s}}|\xi)$. Setting $\vec{\mathbf{s}} = \mathbf{0}$ in it, we have

$$P(\mathbf{0}, \mathbf{0}|\xi) = \frac{1}{N^2(1-\xi)} + \frac{N^2-1}{3N^2} + \varphi_N(\mathbf{0}, 1) + o(1).$$

Using this expression in (29), it follows that

$$\begin{aligned} G^\dagger(N|\xi) &= 1 + \frac{N^2}{N^2-1} \left[\left(\frac{1}{3}(N^2-1) + N^2\varphi_N(\mathbf{0}, 1) \right) (\xi-1) \right. \\ &\quad \left. + \left(\left\{ \frac{1}{3}(N^2-1) + N^2\varphi_N(\mathbf{0}, 1) \right\}^2 \right. \right. \\ &\quad \left. \left. + \left\{ \frac{N^4}{45} - \frac{N^2}{9} + \frac{4}{45} + N^2\varphi_N(\mathbf{0}, 1) \right\} \right) (\xi-1)^2 \right] \\ &\quad + o(\xi-1)^2. \end{aligned} \quad (32)$$

Since $G^\dagger(N|\xi)$ is holomorphic at $\xi = 1$, it is described at this point by its *Taylor's* series. So, differentiating (32) with respect to ξ and taking the limit as $\xi \rightarrow 1^-$ we get Result 4.1. ■

Some general remarks can be drawn from previous results. First, from the first order *Taylor's* series expansion given by (32), the value of $G^\dagger(N|\xi)$ at point $\xi = 1$ is equal to unity, which represents the probability the packet is *ever* trapped by the sink node. This means that the data gathering operation based on URWR is certain. Second, referring to Result 4.1, the mean of System Data Gathering Delay is finite and depends only on N . To study this dependence, $\varphi_N(\mathbf{0}, 1)$ has to be estimated. Two ways are possible. First, $E(\mathcal{D}_N^\dagger)$ is exactly estimated by numerical calculation of $\varphi_N(\mathbf{0}, 1)$. Alternatively the behavior of $E(\mathcal{D}_N^\dagger)$ can be studied by an asymptotic analysis of $\varphi_N(\mathbf{0}, 1)$. Plugging into (30) the asymptotic expansion of $\varphi_N(\mathbf{0}, 1)$ given by (64) in Appendix B, we get the asymptotic expansion of $E(\mathcal{D}_N^\dagger)$ as $N \rightarrow \infty$

$$\begin{aligned} E(\mathcal{D}_N^\dagger) &= \frac{2}{\pi}N^2 \ln(N) + \left(\frac{2}{\pi} \left[\gamma + \frac{1}{2} \ln \left(\frac{2}{\pi^2} \right) + 2\ell_0^{(1)} \right] + \frac{1}{3} \right) N^2 \\ &\quad + \frac{2}{\pi} \ln(N) + \frac{2}{\pi} \left[\gamma + \frac{1}{2} \ln \left(\frac{2}{\pi^2} \right) + 2\ell_0^{(1)} \right] \\ &\quad + \frac{\pi}{18} [1 + 24\ell_1^{(1)}] + O\left(\frac{1}{N^4}\right), \end{aligned} \quad (33)$$

where γ and $\ell_k^{(r)}$ are constants lower than 1 (cf. Appendix B).

Since series $\frac{1}{N^4}$ is fast decreasing, the convergence speed of the approximation given by (33) is quite strong and as shown in Table I, it holds true even for small values of N .

TABLE I
ERROR INDUCED BY THE USE OF APPROXIMATED MEAN AND VARIANCE OF
SYSTEM DELAY RELATIVELY TO EXACT VALUES FOR VARIOUS N

N	Mean Relative Error	Variance Relative Error
3	1.19×10^{-2}	5.22×10^{-2}
5	2.28×10^{-3}	5.45×10^{-2}
10	1.23×10^{-4}	3.88×10^{-2}
30	1.42×10^{-6}	2.14×10^{-2}
100	1.11×10^{-8}	1.24×10^{-2}

3) *Variance of the System Data Gathering Delay* \mathcal{D}_N^\dagger : The variance $V(\mathcal{D}_N^\dagger)$ of \mathcal{D}_N^\dagger is a key parameter as far as quality of service is concerned. It is evaluated in this paragraph.

Result 4.2: If $\varphi_N^{(1)}(\xi, \xi)$ is the first derivative of $\varphi_N(\xi, \xi)$ with respect to ξ , $V(\mathcal{D}_N^\dagger)$ has the closed-form expression

$$V(\mathcal{D}_N^\dagger) = \frac{N^4(N^2 - 2)}{9(N^2 - 1)^2} \left[\{1 + 3\varphi_N(0, 1)\} - \frac{1}{N^2} \right]^2 + \frac{N^6}{(N^2 - 1)} \left[\frac{2}{45} + \frac{[\varphi_N(0, 1) + 2\varphi_N^{(1)}(0, 1)]}{N^2} + \frac{1}{5N^4} \right]^2 \quad (34)$$

Proof: The variance of System Data Gathering Delay is

$$V(\mathcal{D}_N^\dagger) = E((\mathcal{D}_N^\dagger)^2) - (E(\mathcal{D}_N^\dagger))^2 = \lim_{\xi \rightarrow 1^-} \frac{\partial^2}{\partial \xi^2} G^\dagger(N|\xi) + \lim_{\xi \rightarrow 1^-} \frac{\partial}{\partial \xi} G^\dagger(N|\xi) - \left[\lim_{\xi \rightarrow 1^-} \frac{\partial}{\partial \xi} G^\dagger(N|\xi) \right]^2. \quad (35)$$

Then, plugging into (29) the asymptotic expansion of $P(\mathbf{0}, \mathbf{0}|\xi)$ given by (62) provides an asymptotic expansion of $G^\dagger(N|\xi)$ near $\xi = 1$. The limits of the first and second derivative of $G^\dagger(N|\xi)$ are respectively the first-order and the second-order of the series to be used to get (34). ■

Result 4.3: As N increases, $V(\mathcal{D}_N^\dagger)$ verifies

$$V(\mathcal{D}_N^\dagger) \sim \left\{ N^2 \left[\frac{1}{3} + \varphi_N(0, 1) \right] \right\}^2. \quad (36)$$

Proof: In appendix A, it has been shown that, as N increases, $\varphi_N^{(1)}(0, 1) \sim \frac{N^2}{6} \varphi_N(0, 1)$. By substituting this expression in (34), an equivalent for the variance can be derived. Then, since $\varphi_N(0, 1) \sim \frac{2}{\pi} \ln(N)$ according to asymptotic development (64), it can be deduced that the main contribution in the variance comes from the first term of (34) which is equivalent to $\{N^2[\frac{1}{3} + \varphi_N(0, 1)]\}^2$. ■

For various N , Table I compares the approximated variance given by (36) with respect to the exact computation. It indicates that even for small N the approximation makes sense.

Beyond the accuracy of the equivalent (36) of the variance of System Data Gathering delay, it is remarkable that it is just close to the square of its mean (30).

4) *Discussion:* The expression of the mean of System Data Gathering Delay given by (33) is of importance: it captures the

mean behavior of the system and applies for small N . The expression of the variance (34) and the equivalent (36) deduced as N increases, refine the idea designers can have about the QoS of the system. Indeed, first, their expressions also stand even for small values of N . Next, this equivalent of the variance is just the square of the mean. Now, the stochastic process under study consists of a uniform memoryless generation of a walker over the network on which URWR – that is a succession of memoryless processes – applies until the walker is trapped at a collector node. So, the existence of an equivalent of the variance that is just the square of the mean and that holds good for small N let us infer that, as a good approximation, an exponential probability distribution can be assumed for the System Data Gathering Delay. It is thus possible to define the percentile the delay is below a given threshold.

Thus, the results derived from the infinite lattice model give insight of the behavior of wide range systems in which collectors are, in average, regularly spread. Moreover, they allow to properly dimension the scale of the collector distribution while targeting a given level of QoS like the percentile the delay is below a given threshold or the mean delay. This scale can also be interpreted as the typical granularity above which the system should be structured which is known to enhance performance [22].

The results can now be translated into numerical figures for WDCN. As pointed out in II, WDCN gather about 10 bytes information per message from every node. There are a few 100s of nodes. The data gathering should last a few seconds or a few 10s of seconds. The amount of data to be carried at system level is thus about 100 kbits. Hence targeting IEEE802.15.4-like devices that offer 250 kbps at 30 m range the system works then at low load. As a consequence, there is no need to optimize message scheduling nor to implement tight synchronization over the system and basic asynchronous approaches like CSMA/CA to access the medium are quite appropriate. Then, assuming that the physical layer capabilities can ensure full connectivity adapting its coding rate according to the range dispersion for instance, the typical delay to transmit 1 bit per hop equals 4 μ s. Therefore, the time to send a message – the time slot duration – is 320 μ s. This is high enough to neglect the circuits and MAC delays. To gather data from a sensor node within 1 s, in average, the number of hops should not exceed $\bar{n} = 10^6/320 = 3125$. This occurs for scales verifying $N \leq 36$ according to Fig. 2. As discussed above, considering an exponential probability distribution for \mathcal{D}_N^\dagger , deeper characterization of the quality of service can be provided looking at the probability the mean delay is under a given bound. The percentile p , $0 < p < 1$, to be under bound \bar{n} requires to wait $-\bar{n} \ln(1 - p)$. Curves for different p are presented in Fig. 2. Admissible N vary from 58 to 6, i.e., network size varies from 3664 to 36 nodes while System Data Gathering Delay is within 5 s 80% of the time or within 0.1 s 99% of the time respectively. Between, targeting 1 s delay 99% of the time requires $N \leq 18$. It is worth noting that while $p \leq 1 - \frac{1}{e} \simeq 0.63$, delays lower than those given by $E(\mathcal{D}_N^\dagger)$ can often be expected. These figures show that although the performance dispersion is significant, the results are within 1 s up

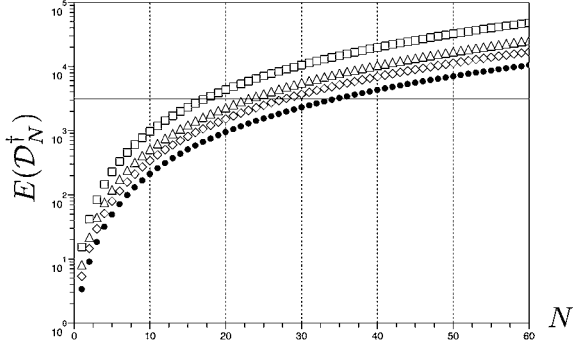


Fig. 2. Mean of system data gathering delay $E(\mathcal{D}_N^\dagger)$ in hop unit (●). As a good approximation, related standard deviation equals the mean. Other curves indicate the delay one has to wait to be sure at 80% (◊), 90% (△) and 99% (□) that the message has hit the sink. The horizontal line marks the 3125 coordinates.

to 10 s for networks with few 10s up to several 100s of nodes. This is fully in range with WDGn requirements.

B. Spatial Distribution of Mean Data Gathering Delay

This paragraph focuses on the spatial properties of the data gathering delay. As mentioned previously, the data gathering delay is the time or the number of hops it takes for a message issued from an arbitrary sensor node $\vec{s} = \{s_1, s_2\}$ to reach the sink at the origin for the first time where it is trapped.

Result 4.4: The spatial behavior of the data gathering delay has the closed-form expression

$$E(\mathcal{D}_N^\dagger(\vec{s})) = N^2[\varphi_N(\vec{0}, 1) - \varphi_N(\vec{s}, 1)] + 2s_2(N - s_2) \quad (37)$$

where $\varphi_N(\vec{s}, \xi)$ is the N -dependent holomorphic function defined by (59) in Appendix A.

Proof: The probability that this message is trapped after n hops is the first-passage probability

$$Pr\{\mathcal{D}_N^\dagger(\vec{s}) = n\} = F_n^\dagger(\vec{s}, 0), \quad n \geq 0.$$

The Mean Data Gathering Delay $E(\mathcal{D}_N^\dagger(\vec{s}))$ is

$$E(\mathcal{D}_N^\dagger(\vec{s})) = \lim_{\xi \rightarrow 1^-} \frac{\partial}{\partial \xi} F^\dagger(\vec{s}, 0 | \xi). \quad (38)$$

Then, substituting (26) in (38) leads to

$$E(\mathcal{D}_N^\dagger(\vec{r})) = \lim_{\xi \rightarrow 1^-} \frac{\partial}{\partial \xi} \frac{P(\vec{r}, \mathbf{0} | \xi)}{P(\mathbf{0}, \mathbf{0} | \xi)}. \quad (39)$$

The asymptotic expansion of the Green function $P(\vec{s}, \mathbf{0} | \xi)$ as $\xi \rightarrow 1$ is given in Appendix A. It can be derived first that

$$P(\mathbf{0}, \vec{0} | \xi) = \frac{1}{N^2(1 - \xi)} + \frac{N^2 - 1}{3N^2} + \varphi_N(\vec{0}, 1) + o(1). \quad (40)$$

So, next, $P(\vec{s}, \mathbf{0} | \xi)/P(\mathbf{0}, \mathbf{0} | \xi)$ can be expanded as

$$\frac{P(\vec{s}, \mathbf{0} | \xi)}{P(\mathbf{0}, \mathbf{0} | \xi)} = 1 + [N^2(\varphi_N(\vec{0}, 1) - \varphi_N(\vec{s}, 1)] + 2s_2(N - s_2)(\xi - 1) + o(\xi - 1). \quad (41)$$

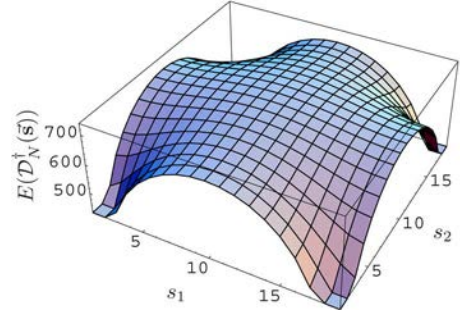


Fig. 3. Spatial distribution of mean delay $E(\mathcal{D}_N^\dagger(\vec{s}))$ in hop unit, for a message originating from sensor at $s = \{s_1, s_2\}$ coordinates on a regular 18×18 square lattice cell to hit one of the collectors located at cell vertices.

$P(\vec{s}, \mathbf{0} | \xi)/P(\mathbf{0}, \mathbf{0} | \xi)$ is holomorphic at $\xi = 1$. Then, differentiating (41) with respect to ξ and setting $\xi = 1$ leads to (37). ■

In (37), the expression $s_2(N - s_2)$ increases for $s_2 < \frac{N}{2}$ and decreases for $s_2 > \frac{N}{2}$. Moreover in Appendix A it has been shown that s_1 and s_2 dependencies of φ_N vary independently and that they decrease for values lower than $\frac{N}{2}$ and increase for values greater than $\frac{N}{2}$. Hence, $E(\mathcal{D}_N^\dagger(\vec{s}))$ has an absolute maximum at $\vec{\frac{N}{2}} = \{\frac{N}{2}, \frac{N}{2}\}$, i.e., in the center of the cell. Here, for even values of N , the maximum delay is

$$E\left(\mathcal{D}_N^\dagger\left(\vec{\frac{N}{2}}\right)\right) = N^2 \left[\varphi_N(\vec{0}, 1) - \varphi_N\left(\vec{\frac{N}{2}}, 1\right) \right] + \frac{N^2}{2}. \quad (42)$$

It is then interesting to compare this maximum with the System Data Gathering Delay given in (33), by evaluating parameter $\Delta_N = E(\mathcal{D}_N^\dagger(\vec{\frac{N}{2}})) - E(\mathcal{D}_N^\dagger)$. Remarking that $\varphi_N(\vec{\frac{N}{2}}, 1) = Q_3^{\frac{1}{2}}(N)$ defined in Appendix B-C and for which an asymptotic expansion has been derived in (78), next, using the asymptotic expansion of $\varphi_N(\vec{0}, 1)$ made explicit in (64), an asymptotic expansion can be found for $E(\mathcal{D}_N^\dagger(\vec{\frac{N}{2}}))$. Then, plugging this latter and the asymptotic expansion (33) of $E(\mathcal{D}_N^\dagger)$ in the expression of Δ_N leads to

$$\Delta_N = N^2 \left[\frac{2}{3} - \frac{4}{\pi} \ell_0^{(\frac{1}{2})} \right] - \frac{2}{\pi} \ln(N) - \frac{2}{\pi} \left[\gamma - \frac{1}{2} \ln\left(\frac{2}{\pi^2}\right) + 2\ell_0^{(1)} \right] - \frac{4\pi}{3} \ell_1^{(\frac{1}{2})} + O\left(\frac{1}{N}\right)^4 \quad (43)$$

1) *Discussion:* The difference Δ_N between the maximum Mean Data Gathering Delay and the System Data Gathering Delay quantifies the dispersion of the delay according to the different locations of the sensor nodes. Relation (43) indicates that it evolves as $\sim 0.61N^2$ while, referring to (36) and (64), the standard deviation of the stochastic process related to the System Data Gathering Delay varies as $\frac{2}{\pi}N^2 \ln(N)$. In other words, at the first order, the dispersion induced by the memoryless property of the URWR transport noticeably exceeds the effect of the spatial dispersion of sensor nodes.

Fig. 3 represents $E(\mathcal{D}_N^\dagger(\vec{s}))$ in hop unit for $N = 18$ which corresponds to a 324 nodes network. At the maximum, the mean

number of hops before the message reaches the sink is 731 corresponding to a 0.23 s delay considering 10 bytes messages at 250 kbps data rate. Under the same conditions, Fig. 2 shows that System Data Gathering Delay corresponds to 661 hops (i.e., 0.21 s) while it has to be waited for 1522 hops, i.e., 0.48 s in order to be able to capture the data message 90% of the cases. Hence, over lattices that have a few hundreds of nodes, the delay dispersion according to sensor location is still relatively low (10% of the System Data Gathering Delay) particularly compared to the variance of URWR stochastic process. Thus performance features are relatively uniform as far as sensor nodes location is concerned.

C. Energy Consumption

The main focus of this paper is to discuss the capability of URWR to lower complexity keeping the lifetime of the system as long as possible. This section examines the latter point by evaluating the contribution of URWR to the power consumption, i.e., the contribution originating from the multiple random receipts and transmissions at the relay nodes. In this context, the mean number of hops $E(\mathcal{D}_N^\dagger)$ a message that carries one data unit undergoes before hitting a collector gives a measure of the mean contribution of URWR to the energy consumption. However, dealing with long life time systems, to evaluate possible burning node effects for example, the spatial distribution of the energy consumption is also of key interest.

1) *Mean Number of Visits of a Packet at a Sensor Node:* At a relay node \vec{s} , the contribution of URWR to the energy consumption is proportional to the number of visits of a message walker.

Result 4.5: The mean number of visits of a packet to sensor node \vec{s} before being trapped at a sink node is

$$\mathcal{E}^\dagger(\vec{s}) = \frac{1}{(N^2 - 1)} \lim_{\xi \rightarrow 1^-} \left\{ \frac{1}{1 - \xi} \left(1 - \frac{P(\mathbf{0}, \vec{s} | \xi)}{P(\mathbf{0}, \mathbf{0} | \xi)} \right) \right\}. \quad (44)$$

Proof: Let us define at sensor node \vec{s} the random variable $I_n(\vec{s})$, which takes the value 1 if sensor node \vec{s} is visited by the packet on the n th hop, and zero otherwise. Denoting $H_n^\dagger(\vec{s})$ and $H^\dagger(\vec{s} | \xi)$ the probability and related generating function respectively that sensor node \vec{s} is visited at hop n , we have

$$Pr\{I_n(\vec{s}) = 1\} = H_n^\dagger(\vec{s}).$$

The number of times sensor node \vec{s} is visited during the walk is nothing but the random variable $\sum_{n=0}^{\infty} I_n(\vec{s})$ whose expectation (mean number of visits) can be derived as follows:

$$\begin{aligned} \mathcal{E}^\dagger(\vec{s}) &= E \left(\sum_{n=0}^{\infty} I_n(\vec{s}) \right) = \sum_{n=0}^{\infty} E(I_n(\vec{s})) \\ &= \sum_{n=0}^{\infty} H_n^\dagger(\vec{s}) = \lim_{\xi \rightarrow 1^-} H^\dagger(\vec{s} | \xi). \end{aligned}$$

Now, it remains to make explicit generating function $H^\dagger(\vec{s} | \xi)$. Using the law of total probability, it is possible to decompose the event that a packet generated at any sensor node will visit sensor node \vec{s} on the n th hop, which has the probability $H_n^\dagger(\vec{s})$, into the $N^2 - 1$ mutually exclusive events

that the packet is initially generated at sensor node \vec{r} with probability $\frac{1}{N^2 - 1}$, and then visits sensor node \vec{s} after n hops, which occurs with probability $P_n^\dagger(\vec{r}, \vec{s})$. Thus, we obtain

$$H_n^\dagger(\vec{s}) = \frac{1}{N^2 - 1} \sum_{\vec{r} \neq \mathbf{0}} P_n^\dagger(\vec{r}, \vec{s}).$$

Multiplying both sides by ξ^n , summing over all n , we get

$$H^\dagger(\vec{s} | \xi) = \frac{1}{N^2 - 1} \sum_{\vec{r} \neq \mathbf{0}} P^\dagger(\vec{r}, \vec{s} | \xi). \quad (45)$$

However, from Theorem (3.1), $P^\dagger(\vec{r}, \vec{s} | \xi)$ can be expressed

$$P^\dagger(\vec{r}, \vec{s} | \xi) = P(\vec{r}, \vec{s} | \xi) - P(\mathbf{0}, \vec{s} | \xi) \frac{P(\vec{r}, \mathbf{0} | \xi)}{P(\mathbf{0}, \mathbf{0} | \xi)}, \quad \vec{r}, \vec{s} \neq \mathbf{0}. \quad (46)$$

Then, plugging (46) into (45), using the symmetric property of $P(\vec{r}, \vec{s} | \xi)$ rendered by (12) and normalization condition (3), $H^\dagger(\vec{s} | \xi)$ can be rewritten as

$$H^\dagger(\vec{s} | \xi) = \frac{1}{(N^2 - 1)(1 - \xi)} \left(1 - \frac{P(\mathbf{0}, \vec{s} | \xi)}{P(\mathbf{0}, \mathbf{0} | \xi)} \right). \quad (47)$$

By taking the limit of both sides of (47) as $\xi \rightarrow 1$ (through real values) from below, we obtain (44). ■

Result 4.5 does not provide an explicit expression of the mean number of visits. However, it is possible to infer a closed-form by expanding function $H^\dagger(\vec{s} | \xi)$ close to $\xi = 1^-$. Indeed, since the mean number of visits is defined as the limit of function $H^\dagger(\vec{s} | \xi)$ as $\xi \rightarrow 1^-$, a zero-order *Taylor's* series expansion of $H^\dagger(\vec{s} | \xi)$ with the point of expansion $\xi = 1$ is sufficient to obtain an explicit formula.

Result 4.6: The mean number of visits of a packet to sensor node \vec{s} before being trapped at a sink node has the closed-form

$$\mathcal{E}^\dagger(\vec{s}) = \frac{N^2}{N^2 - 1} [\varphi_N(\mathbf{0}, 1) - \varphi_N(\vec{s}, 1)] + \frac{2s_2(N - s_2)}{N^2 - 1}, \quad (48)$$

$\varphi_N(\vec{s}, \xi)$ being the function defined by (59) in Appendix A.

Proof: The asymptotic expansion of $P(\mathbf{0}, \vec{s} | \xi)$ as $\xi \rightarrow 1^-$ (62), is established in Appendix A. From it, it can be deduced that $P(\mathbf{0}, \vec{s} | \xi)/P(\mathbf{0}, \mathbf{0} | \xi)$ is holomorphic, and hence, it can be represented by its first-order *Taylor's* series expansion with the point of expansion $\xi = 1$ as follows:

$$\begin{aligned} \frac{P(\mathbf{0}, \vec{s} | \xi)}{P(\mathbf{0}, \mathbf{0} | \xi)} &= 1 + N^2 [\varphi_N(\mathbf{0}, 1) - \varphi_N(\vec{s}, 1)] \\ &\quad + 2s_2(N - s_2) \times (\xi - 1) + o(\xi - 1). \end{aligned} \quad (49)$$

Plugging (49) into (47), taking the limit as $\xi \rightarrow 1^-$, provides Result 4.6. ■

2) *Discussion:* Some general remarks can be drawn from Result 4.6. First, the mean number of visits and the mean Data Gathering Delay are related to each other as follows:

$$\mathcal{E}^\dagger(\vec{s}) = \frac{E(\mathcal{D}_N^\dagger(\vec{s}))}{N^2 - 1}. \quad (50)$$

This can be explained by the fact that with a uniform traffic distribution, fraction $E(\mathcal{D}_N^\dagger(\vec{s}))/ (N^2 - 1)$ represents the *space*

TABLE II
MEAN PERFORMANCE OF URWR, SPR, A-URWR AND A-SPR FOR 10 BYTES
MESSAGE SENT AT 250 KBPS ON A 18×18 SQUARE LATTICE

Scheme	Hop Weight	Delay (s)	Number of Visits	Visited Fraction
SPR	9	$2.88 \cdot 10^{-3}$	0.07	0.07
URWR	661	0.21	2.04	0.76
A-SPR	2907	0.93	1	1
A-URWR	$843 \cdot 10^2$	≤ 26.97	2.04	0.76

average number of visits of a packet issued from sensor node \vec{s} to each sensor node in the network. In particular, this represents also the space average number of returns of the packet to the initial sensor node \vec{s} . However, $\mathcal{E}^\dagger(\vec{s})$ represents the *time* average number of visits of a packet issued anywhere in the network to the sensor node \vec{s} . Therefore, the equality between the space average number of returns, $E(D_N^\dagger(\vec{s})) / (N^2 - 1)$, and the time average number of visits, $\mathcal{E}^\dagger(\vec{s})$, expresses simply the *ergodicity* property of the system.

Second, note that the mean number of visits depends on both the scale N of the network and the position of sensor node \vec{s} . This is predictable since the sensor nodes in the vicinity of the sink node are not equivalent to those in the middle of the cell. However, looking at (50) and the closed-form expression of Δ_N given by (43) it can be deduced that the spatial deviation of $\mathcal{E}^\dagger(\vec{s})$ with respect to the mean number of visits described by $E(D_N^\dagger) / (N^2 - 1)$ varies slowly in a few units range. Hence, URWR achieves to approach quite well the *uniform* load balancing property throughout the network.

Moreover, from (50) one can observe that like $E(D_N^\dagger(\vec{s}))$, $\mathcal{E}^\dagger(\vec{s})$ has an absolute maximum in the center of the cell. The asymptotic expansion of $\mathcal{E}^\dagger(\vec{s})$ at this maximum can be evaluated. Since $\varphi_N(\frac{\vec{N}}{2}, 1) = Q_{\frac{2}{3}}^{\frac{2}{3}}(N)$ for which an asymptotic expansion has been derived in (78), plugging this latter and the asymptotic expansion (64) of $\varphi_N(\vec{0}, 1)$ in (42), one finds

$$\mathcal{E}^\dagger\left(\frac{\vec{N}}{2}\right) \sim \frac{2}{\pi} \ln(N) + \frac{1}{2} + \frac{2}{\pi} \left[\gamma + \frac{1}{2} \ln\left(\frac{2}{\pi^2}\right) + 2(\ell_0^{(1)} - \ell_0^{(\frac{1}{2})}) \right] + O\left(\frac{1}{N^4}\right).$$

Then, another conclusion is that over the scales of interest ($N \in [3, 33]$), the mean number of visits increases slowly with N and remains in the $[1.33, 2.51]$ range. For example, back to a 18×18 network, from Fig. 3 on which (50) is applied, the maximum mean number of visits equals to $731/323 = 2.26$ in the center of the cell against a mean number of visits averaged over the system that equals $661/323 = 2.04$.

V. GENERAL DISCUSSION

In the previous paragraph, the performance of URWR to carry a message from a source to a sink have been quantified in terms of delay and power consumption. It has been shown that as far as typical sink density of WDGn is concerned, though dispersive, URWR scheme fulfils the delay requirements. Futhermore, it

has been shown that URWR achieves good load balancing properties. Now, URWR figures can be interestingly compared to the figures of deterministic routing schemes. For instance, applying Shortest Path Routing (SPR) on same square lattice model, the delay to transmit a message from a source to the closest sink at the origin, is $s_1 + s_2$ and if N is odd, the mean delay D_{SPR}^\dagger is

$$D_{SPR}^\dagger = \frac{4}{(N-1)^2} \sum_{0 \leq s_1 \leq \frac{N-1}{2}, 1 \leq s_2 \leq \frac{N-1}{2}} s_1 + s_2 = \frac{N}{2}.$$

D_{SPR}^\dagger also gives a measure of the energy consumption induced by SPR protocol. At a sensor node, the averaged power consumption $\mathcal{E}_{SPR}^\dagger$ can be expressed as

$$\mathcal{E}_{SPR}^\dagger = \frac{D_{SPR}^\dagger}{(N^2 - 1)} = \frac{N}{2(N^2 - 1)}.$$

Thus, for a 10 bytes message transmitted at 250 kbps on a 18×18 lattice, as presented in Table II, D_{SPR}^\dagger equals 9 hops against 661 for URWR. This leads to a delay that is 2.88 ms while we have to wait 0.21 s in average for URWR or even up to 1 s to get the information 99% of the time. Then, in terms of mean delay and mean contribution to the energy consumption, URWR is about 30 times less efficient than SPR.

Now, a point is that beyond the data retrieval from a given sensor node, WDGn aim at gathering information from the overall set of sensor nodes to get a general overview of the evolution of the physical parameters over the covered area. In multihop networks, retrieval paths from different sensors have a significant fraction of links in common. Hence the better option may not be to generate as many messages as there are sensors nodes. Aggregation can particularly suited at least to reduce overheads or collision management efforts. We call this scheme A-URWR for Aggregating URWR.

Using A-URWR, reminding that the mean number of visits at any node is close to unity, it appears that, in average, just 1 message walker would be sufficient to scan a significant part of the sensor nodes. To get deeper insight on this property, the mean number of distinct nodes the message visits before being trapped at a collector can be evaluated. It is the mean number S_n of distinct nodes a random walker has visited on a square lattice with no trapping site after n steps. It has been shown that for $n > 7$, $\frac{2\pi n}{1.066\pi - 1 + \ln(n)} > S_{2n-1} > \frac{2\pi n}{1.16\pi - 1 + \ln(n)}$ [20].

Applying this result, on a 18×18 square lattice, since $E(D_N^\dagger)$ equals 661, there are at least 246 distinct nodes visited in average. This corresponds to 76% of the nodes contained in a cell. So, here, the generation of 1 aggregating message walker per cell allows to gather data from a large majority of sensor nodes. It is to be noted that the aggregation of sensor data in a single message walker is formally equivalent with respect to the delay to the gathering of data by means of a mobile sink as introduced in [23].

Using aggregation, the performance of data gathering over the network can be estimated summing the numbers d of data units carried at each hop h over the set of paths p . One gets the estimator $W^\dagger = \sum_p \sum_h d_{p,h}$. Just 1 message, i.e., 1 path, is necessary to scan a significant part of the network. Futhermore,

while aggregating, the mean message size is half its maximum size. Considering that, at most, the message contains as many data units there are distinct visited nodes, one has

$$W_{URWR}^\dagger = \frac{S_{E(D^\dagger)} E(D^\dagger)}{2}. \quad (51)$$

Dealing with Aggregating-SPR (A-SPR), it comes that

$$W_{SPR}^\dagger = 2 \times 2N \sum_{0 \leq s \leq \frac{(N-1)}{2}} s = \frac{1}{2} N(N^2 - 1). \quad (52)$$

It is just the number of sensor nodes times the mean delay. Then, assuming 10 bytes data units transmitted at 250 kbps on a 18×18 lattice, as presented in Table II, the delay to convey the aggregated data from the source to a collector is 0.93 s and 26.02 s for A-SPR and A-URWR respectively. Thus, as compared to SPR approach, URWR with aggregation reduces by a factor 2 the loss of performance. Note that increasing the density of collectors by 4.6 reduces the relative loss to a factor about 10 (9.92) and allows URWR to perform as SPR.

Until now, the analysis has focused on the impact of the collector–sensor nodes ratio. For the designer, it indicates how it has to be adjust to meet a given level of performance. However, upon URWR, enriched design can also be built up to modulate further the performance at system level. For instance, the generation of $m \geq 1$ independent message walkers can be envisioned. This would geometrically increase the mean fraction of visited sensors at each gathering cycle, and meaningfully reduce the presence of gaps in the collected data set at

limited energy consumption increase. Indeed, if $\rho_N = \frac{E(D_N^\dagger)}{(N^2-1)}$ is the fraction of visited node by a message, the total fraction of visited nodes is $1 - (1 - \rho_N)^m$ and the energy consumption varies as $\rho_N \sum_{q=1}^m (1 - \rho_N)^{q-1}$. For $m = 2$, about 95% of the nodes would have been visited with 30% energy expense increase. Multiple generation would also decrease typical delay since with 0.63 probability, the delay is lower than typical System Data Gathering Delay as discussed in Section IV-A2 and since the data payload would be distributed among independent messages that would thus be shorter. The generation of several walkers could happen in a stochastic way in order to keep with no-knowledge schemes or upon some data buffers or timers status. Second, since the extension of the delay for a message while enabling aggregation along the random walk of the message walker is high compared to the case without aggregation, activating aggregation or not or up to a certain extend would be of interest. This would just require the presence of a dedicated flag in the message header for instance. Thus, gathering schemes based on URWR could provide different levels of latency. These features are under investigation and their analysis will be provided in an independent paper.

VI. CONCLUSION

In this paper it has been pointed out that the scale of WDGn is quite small and that the required quality of service can be significantly relaxed compared to what is usually expected from wireless sensor networks. These relaxed constraints make room

for rough protocols. Then, to reduce the cost by reducing complexity, operation modes based on low or even no system knowledge have been discussed. In particular, a stateless random walk option as routing scheme has been revisited. The typical quality of service parameters such as delay, spatial properties and energy consumption have been examined with special attention to asymptotic behaviors by providing analytical expressions valid even for small scale systems. From the analysis of these expressions, the properties of unicast random walk routing have been derived. The performance as compared to deterministic approaches like shortest path routing has been quantified in terms of delay and energy consumption. Data gathering schemes at system level that fulfil the WDGn requirements in terms of delay with sustainable energy consumption have been proposed.

Results have been obtained in the light of the random walk theory. We have considered basic assumptions since our focus was to capture the properties of pure and simple random routing. So, edge effects, interdistance node dispersion, non-planar topologies, interference or the impact of medium access control protocols have not been addressed. However, the random walk theory provides tools that could be used to enrich our model. For example, the modification of the combinatory induced by the edges can be taken into account by introducing a finite lattice with appropriate boundary conditions. Parameters like interdistance node dispersion, non-planarity or interference can be handled until a certain degree of regularity is identified. Otherwise, effects inducing time inhomogeneity like collisions at the medium access control level can be analyzed by extending the discrete random walk to the time continuous random walk. Thus, beyond the applicability of low-knowledge based schemes for small scale systems, like in joint optimized routing and data gathering in WDGn, the model this paper defines can also be viewed as a first step to be enriched, to statistically model and understand networks with a high number of degrees of freedom and from which a direct handling of the geographic position is of importance.

APPENDIX A

ASYMPTOTIC ANALYSIS OF $P(\mathbf{0}, \vec{s} | \xi)$ CLOSE TO $\xi = 1$

Singularity of $P(\mathbf{0}, \vec{s} | \xi)$ at $\xi = 1$: Here the expression of generating function $P(\mathbf{0}, \vec{s} | \xi)$ is simplified and its singularity at point $\xi = 1$ is studied.

From the expression (15) of $P(\mathbf{0}, \vec{s} | \xi)$, factorizing the denominator of the summand and using the addition theorems of trigonometric functions, we obtain

$$\begin{aligned} P(\mathbf{0}, \vec{s} | \xi) &= \frac{1}{N^2} \sum_{m_1, m_2=0}^{N-1} \left\{ \frac{e^{-i \frac{2\pi}{N} m_1 s_1}}{1 - \frac{\xi}{2} \cos(\frac{2\pi}{N} m_1)} \times \frac{e^{-i \frac{2\pi}{N} m_2 s_2}}{1 - c_{m_1}(\xi) \cos(\frac{2\pi}{N} m_2)} \right\} \\ &= \frac{1}{N^2} \sum_{m_1=0}^{N-1} \frac{e^{-i \frac{2\pi}{N} m_1 s_1}}{1 - \frac{\xi}{2} \cos(\frac{2\pi}{N} m_1)} \times \mathcal{S}_{m_1}(\xi) \end{aligned} \quad (53)$$

where functions $c_{m_1}(\xi)$ and $\mathcal{S}_{m_1}(\xi)$ are defined as

$$c_{m_1}(\xi) = \frac{\xi}{2 - \xi \cos(\frac{2\pi}{N} m_1)} \quad (54a)$$

$$\mathcal{S}_{m_1}(\xi) = \sum_{m_2=0}^{N-1} \frac{e^{-i \frac{2\pi}{N} m_2 s_2}}{1 - c_{m_1}(\xi) \cos(\frac{2\pi}{N} m_2)}. \quad (54b)$$

To simplify $\mathcal{S}_{m_1}(\xi)$, the first step is to note from (54a) that $0 < |c_{m_1}(\xi)| < 1$ for $0 < \xi < 1$. Hence, using the exponential representation of cos function, $\mathcal{S}_{m_1}(\xi)$ can be rewritten as

$$\mathcal{S}_{m_1}(\xi) = -\frac{2}{c_{m_1}(\xi)} \cdot \sum_{m_2=0}^{N-1} \left\{ \frac{e^{i\frac{2\pi}{N}m_2(1-s_2)}}{e^{i\frac{2\pi}{N}m_2} - \alpha_{m_1}(\xi)} \times \frac{1}{e^{i\frac{2\pi}{N}m_2} - \alpha_{m_1}^{-1}(\xi)} \right\}.$$

$\alpha_{m_1}(\xi)$ is the smallest root of $X^2 - \frac{2}{c_{m_1}(\xi)}X + 1 = 0$ whose discriminant is nonnegative. Thus, we find

$$\alpha_{m_1}(\xi) = \left(1 - \sqrt{1 - c_{m_1}^2(\xi)}\right) / c_{m_1}(\xi). \quad (55)$$

Using partial fraction decomposition, we can write $\mathcal{S}_{m_1}(\xi)$ as

$$\mathcal{S}_{m_1}(\xi) = (1 - c_{m_1}^2(\xi))^{-\frac{1}{2}} \cdot \sum_{m_2=0}^{N-1} \left\{ \frac{e^{-i\frac{2\pi}{N}m_2s_2}}{1 - \alpha_{m_1}(\xi)e^{-i\frac{2\pi}{N}m_2}} + \frac{\alpha_{m_1}(\xi)e^{i\frac{2\pi}{N}m_2(1-s_2)}}{1 - \alpha_{m_1}(\xi)e^{i\frac{2\pi}{N}m_2}} \right\}.$$

Noting that $|\alpha_{m_1}(\xi)| < 1$, it is then possible to expand each sum involved in $\mathcal{S}_{m_1}(\xi)$ by using successively the expansion $\frac{1}{(1-x)} = \sum_{k=0}^{\infty} x^k$ and the identity

$$\sum_{m=0}^{N-1} e^{i\frac{2\pi}{N}mn} = \begin{cases} N & \text{for } n = 0, \pm N, \pm 2N, \dots \\ 0 & \text{otherwise,} \end{cases}$$

which can be derived by remarking that the vectors $e^{i\frac{2\pi}{N}mn}$ form an orthogonal basis over the set of N -dimensional complex vectors. Therefore, we obtain

$$\mathcal{S}_{m_1}(\xi) = \frac{N}{(1 - c_{m_1}^2(\xi))^{\frac{1}{2}}} \times \frac{\alpha_{m_1}^{s_2}(\xi) + \alpha_{m_1}^{N-s_2}(\xi)}{1 - \alpha_{m_1}^N(\xi)}. \quad (56)$$

Finally, by substituting (56) into (53), we obtain

$$P(\mathbf{0}, \vec{s} | \xi) = \frac{1}{N} \sum_{m_1=0}^{N-1} \left\{ \frac{e^{-i\frac{2\pi}{N}m_1s_1}}{(1 - \xi \cos(\frac{2\pi}{N}m_1))(1 - c_{m_1}^2(\xi))^{\frac{1}{2}}} \times \frac{\alpha_{m_1}^{s_2}(\xi) + \alpha_{m_1}^{N-s_2}(\xi)}{1 - \alpha_{m_1}^N(\xi)} \right\} \quad (57)$$

Remark that the summand involved in (57) is holomorphic over $0 < \xi < 1$ for all $0 \leq m_1 \leq N-1$. However, it diverges at $\xi = 1$ when $m_1 = 0$. Thus, the singularity of $P(\mathbf{0}, \vec{s} | \xi)$ at $\xi = 1$ comes only from the first term of the sum given by (57). It is convenient therefore to separate out this singular part from the non-singular parts denoted $\varphi_N(\vec{s}, \xi)$ of $P(\mathbf{0}, \vec{s} | \xi)$

$$P(\mathbf{0}, \vec{s} | \xi) = \frac{1}{N(1 - \xi)^{\frac{1}{2}}} \times \frac{\alpha_0^{s_2}(\xi) + \alpha_0^{N-s_2}(\xi)}{1 - \alpha_0^N(\xi)} + \varphi_N(\vec{s}, \xi) \quad (58)$$

with

$$\varphi_N(\vec{s}, \xi) = \frac{1}{N} \sum_{m_1=1}^{N-1} \left\{ \frac{e^{-i\frac{2\pi}{N}m_1s_1}}{(1 - \xi \cos(\frac{2\pi}{N}m_1))(1 - c_{m_1}^2(\xi))^{\frac{1}{2}}} \times \frac{\alpha_{m_1}^{s_2}(\xi) + \alpha_{m_1}^{N-s_2}(\xi)}{1 - \alpha_{m_1}^N(\xi)} \right\}. \quad (59)$$

Looking at $\varphi_N(\vec{s}, \xi)$ expression, considering m_1 terms in pair with $N - m_1$ terms, it can be remarked that the imaginary parts cancel out and noting that if $m_1 = \frac{N}{2}$ exists, $\sin(\frac{2\pi}{N}m_1) = 0$, then in any case, $\varphi_N(\vec{s}, \xi)$ is simply real.

Otherwise, from (59), spatial behavior of φ_N can be put in light. s_1 dependency of φ_N varies as $\cos(\frac{2\pi}{N}s_1)$ i.e., is even with respect to line $m_1 = \frac{N}{2}$, decreasing for $s_1 < \frac{N}{2}$ and increasing for $s_1 > \frac{N}{2}$. Since in our model, the two dimensions are studied indiscriminately, s_1 and s_2 can be exchanged, and the same behavior is expected for s_2 . This can be verified studying the s_2 dependency in (59). Because \vec{s} components vary independently in φ_N , it can be concluded that φ_N has an absolute minimum at $\vec{s} = \{\frac{N}{2}, \frac{N}{2}\}$.

Now, dealing with the behavior of φ_N according to ξ , as mentioned above φ_N is holomorphic. Its first derivative $\varphi_N^{(1)}$ with respect to ξ can be calculated from φ_N . Indeed, remarking that ξ dependencies of φ_N appear at the denominator or in powered function at the numerator, $\varphi_N^{(1)}$ can be factorized by φ_N and we find (60), shown at the bottom of the page. From (60), an equivalent of the ratio can be derived at $\xi = 1$.

Let us look at the first term of the summand. Since one has $0 < \xi < 1$, $0 < a_{m_1}(\xi) < 1$ and $0 < \alpha_{m_1}(\xi) < 1$ for all $0 \leq m_1 \leq N-1$, then, the first term vanishes exponentially towards zero as N increases.

Dealing with the second term of the summand, the m_1 dependency is even with respect to line $\frac{N}{2}$, continuous and decreasing over $[\frac{N}{2}, N[$. Then, applying the integral test on this restricted set $[\frac{N}{2}, N[$ primitive being $-m_1 + \frac{2N}{\sqrt{3}\pi} \text{atan}[\sqrt{3}\frac{\pi}{N}m_1]$, it can be shown that the sum of the second term over this set converges and the equivalent $N(\frac{1}{\sqrt{3}} - 1)$ can be derived. Coming back to the overall sum over $[1, N-1]$, $N(\frac{2}{\sqrt{3}} - 1)$ is an equivalent.

The third term can be expressed as

$$b_{m_1} = \frac{-2}{[1 - \cos(x)][2 - \cos(x)][3 - \cos(x)]}$$

with x standing for $\frac{2\pi m_1}{N}$. The singularity of b_{m_1} for $\cos(\cdot) = 1$ indicates that the main contribution of the sum of the third term comes from small values of $\frac{2\pi m_1}{N}$. Then summing the expansion in series of this second term around these small values provides an approximation that captures the essential of the behavior. The expansion in series leads to $\frac{-N^2}{2\pi^2 m_1^2} + \frac{4}{3} + o(\frac{2\pi m_1}{N})^2$ and approximating the sum over $m_1 \in [1, N-1]$ by twice the infinite sum for the first term, which is all the more true as N is high, we find

$$\frac{\varphi_N^{(1)}(\vec{0}, \xi)}{\varphi_N(\vec{0}, \xi)} = - \sum_{m_1=1}^{N-1} \left[\frac{N\alpha_{m_1}(\xi)2^{N-1}\alpha'_{m_1}(\xi)}{1 - \alpha_{m_1}(\xi)^{2N}} + \frac{\cos(\frac{2\pi}{N}m_1)}{2 - \xi \cos(\frac{2\pi}{N}m_1)} + \frac{\alpha'_{m_1}(\xi)\alpha_{m_1}(\xi)}{1 - \alpha_{m_1}(\xi)^2} \right] \quad (60)$$

that $\sum b_{m_1} \sim \frac{N^2}{6} - \frac{4}{3}(N-1)$. Finally, it can be deduced that as N goes toward infinity

$$\frac{\varphi_N^{(1)}(\vec{\mathbf{0}}, 1)}{\varphi_N(\vec{\mathbf{0}}, 1)} \sim \frac{N^2}{6} \quad \text{or} \quad \varphi_N^{(1)}(\vec{\mathbf{0}}, 1) \sim \frac{N^2}{6} \varphi_N(\vec{\mathbf{0}}, 1). \quad (61)$$

Asymptotic Expansion $P(\mathbf{0}, \vec{\mathbf{s}} | \xi)$ as $\xi \rightarrow 1$: To obtain the asymptotic expansion of $P(\mathbf{0}, \vec{\mathbf{s}} | \xi)$ as $\xi \rightarrow 1$, let us successively expand the first term of $P(\mathbf{0}, \vec{\mathbf{s}} | \xi)$ involved in (58) and then function $\varphi_N(\vec{\mathbf{s}}, \xi)$ close to $\xi = 1$. After expanding function $\alpha_0(\xi)$, it can be deduced that

$$\frac{1}{N(1-\xi)^{\frac{1}{2}}} \times \frac{\alpha_0^{s_2}(\xi) + \alpha_0^{N-s_2}(\xi)}{1 - \alpha_0^N(\xi)} = \frac{1}{N^2(1-\xi)} + \frac{N^2 - 6Ns_2 + 6s_2^2 - 1}{3N^2} + o((1-\xi)^{\frac{1}{2}}).$$

Using now the *Taylor's Theorem*, $\varphi_N(\vec{\mathbf{s}}, \xi)$ can be represented by its zero-order *Taylor series expansion* at point $\xi = 1$

$$\varphi_N(\vec{\mathbf{s}}, \xi) = \varphi_N(\vec{\mathbf{s}}, 1) + o((1-\xi)^{\frac{1}{2}}).$$

Finally, combining this asymptotic expansion with the one of the first term of $P(\mathbf{0}, \vec{\mathbf{s}} | \xi)$, we obtain

$$P(\mathbf{0}, \vec{\mathbf{s}} | \xi) = \frac{1}{N^2(1-\xi)} + \frac{N^2(1 + 3\varphi_N(\vec{\mathbf{s}}, 1)) - 6Ns_2 + 6s_2^2 - 1}{3N^2} + o((1-\xi)^{\frac{1}{2}}). \quad (62)$$

APPENDIX B

ASYMPTOTIC EXPANSION OF $\varphi_N(\mathbf{0}, 1)$ AS $N \rightarrow \infty$

Setting $\vec{\mathbf{s}} = \mathbf{0}$ and $\xi = 1$ in (59), we obtain after simplification

$$\varphi_N(\mathbf{0}, 1) = \frac{1}{N} \sum_{m_1=1}^{N-1} \frac{(1 + \alpha_{m_1}^N(1))(1 - \alpha_{m_1}^N(1))^{-1}}{\sin(\frac{\pi}{N}m_1)(1 + \sin^2(\frac{\pi}{N}m_1))^{\frac{1}{2}}}. \quad (63)$$

In this section, we will show that series $\varphi_N(\mathbf{0}, 1)$ has the following asymptotic expansion as $N \rightarrow \infty$

$$\varphi_N(\mathbf{0}, 1) = \frac{2}{\pi} \ln(N) + \frac{2}{\pi} \left(\gamma + \frac{1}{2} \ln\left(\frac{2}{\pi^2}\right) + 2\ell_0^{(1)} \right) + \frac{\pi}{18N^2} (1 + 24\ell_1^{(1)}) + O\left(\frac{1}{N^4}\right) \quad (64)$$

where γ is the *Euler constant* ($\gamma = 0.577215664901$), and $\ell_0^{(1)}$, $\ell_1^{(1)}$ are two constants

$$\ell_0^{(1)} = 0.001872682450 \quad \text{and} \quad \ell_1^{(1)} = 0.009987520718.$$

This asymptotic expansion is obtained by writing

$$\varphi_N(\mathbf{0}, 1) = Q_1(N) + Q_2(N) + Q_3(N), \quad \text{where} \quad Q_1(N) = \frac{1}{N} \sum_{m_1=1}^{N-1} \frac{1}{\sin(\frac{\pi}{N}m_1)},$$

$$Q_2(N) = \frac{1}{N} \sum_{m_1=1}^{N-1} \frac{(1 + \sin^2(\frac{\pi}{N}m_1))^{-\frac{1}{2}} - 1}{\sin(\frac{\pi}{N}m_1)},$$

$$Q_3(N) = \frac{2}{N} \sum_{m_1=1}^{N-1} \frac{\alpha_{m_1}^N(1)(1 - \alpha_{m_1}^N(1))^{-1}}{\sin(\frac{\pi}{N}m_1)(1 + \sin^2(\frac{\pi}{N}m_1))^{\frac{1}{2}}}$$

and then evaluating the asymptotic expansion of each sum.

Asymptotic Expansion of $Q_1(N)$ as $N \rightarrow \infty$: Let $f(x)$, x real, be the function defined as

$$f(x) = \begin{cases} \frac{1}{\sin(x)} - \frac{1}{x} - \frac{1}{\pi-x}, & x \in]0, \pi[\\ -\frac{1}{\pi}, & x = 0, \pi. \end{cases}$$

We can show that f is indefinitely differentiable, in particular

$$f^{(1)}(0) = \frac{1}{6} - \frac{1}{\pi^2} \quad \text{and} \quad f^{(1)}(\pi) = -\frac{1}{6} + \frac{1}{\pi^2}.$$

Remark also that $Q_1(N)$ can be expressed as

$$Q_1(N) = \frac{1}{N} \sum_{m=1}^{N-1} f\left(\frac{\pi}{N}m\right) + \frac{2}{\pi} \sum_{m=1}^{N-1} \frac{1}{m}. \quad (65)$$

Therefore, using the *Euler-Maclaurin summation formula* [21]

$$\frac{1}{N} \sum_{m=1}^{N-1} h\left(\frac{\pi}{N}m\right) = \frac{1}{\pi} \int_0^\pi h(x) dx - \frac{1}{2N} (h(\pi) + h(0)) + \frac{\pi}{12N^2} (h^{(1)}(\pi) - h^{(1)}(0)) + O\left(\frac{1}{N^4}\right). \quad (66)$$

where h is an indefinitely differentiable function, and since $\int_0^\pi f(x) dx = 2 \ln\left(\frac{2}{\pi}\right)$, we obtain

$$\frac{1}{N} \sum_{m=1}^{N-1} f\left(\frac{\pi}{N}m\right) = \frac{2}{\pi} \ln\left(\frac{2}{\pi}\right) + \frac{1}{N\pi} - \frac{\pi}{6N^2} \left(\frac{1}{6} - \frac{1}{\pi^2}\right) + O\left(\frac{1}{N^4}\right). \quad (67)$$

Now, it remains to expand the second sum in (65). It can be recognized as the *Harmonic series* $H_N = \sum_{m=1}^{N-1} \frac{1}{m}$. According to [21], H_N has the following asymptotic expansion

$$H_N = \ln(N) + \gamma - \frac{1}{2N} - \frac{1}{12N^2} + O\left(\frac{1}{N^4}\right), \quad (68)$$

where γ is the *Euler constant*. By plugging (67) and (68) into (65), we find

$$Q_1(N) = \frac{2}{\pi} \ln(N) + \frac{2}{\pi} \left(\gamma + \ln\left(\frac{2}{\pi}\right) \right) - \frac{\pi}{36N^2} + O\left(\frac{1}{N^4}\right). \quad (69)$$

Asymptotic Expansion of $Q_2(N)$ as $N \rightarrow \infty$: Let $g(x)$, x real, be the function defined as

$$g(x) = \begin{cases} \frac{(1 + \sin^2(x))^{-\frac{1}{2}} - 1}{\sin(x)}, & x \in]0, \pi[\\ 0, & x = 0, \pi. \end{cases}$$

We can show that g is indefinitely differentiable, in particular

$$g^{(1)}(0) = -\frac{1}{2} \quad \text{and} \quad g^{(1)}(\pi) = \frac{1}{2}.$$

Note that $Q_2(N)$ can be expressed as

$$Q_2(N) = \frac{1}{N} \sum_{m=1}^{N-1} g\left(\frac{\pi}{N}m\right).$$

Using once again the *Euler-Maclaurin* formula, we get

$$\begin{aligned} \frac{1}{N} \sum_{m=1}^{N-1} g\left(\frac{\pi}{N}m\right) &= \frac{1}{\pi} \int_0^\pi g(x) dx - \frac{1}{2N} (g(\pi) + g(0)) \\ &\quad + \frac{\pi}{12N^2} (g^{(1)}(\pi) - g^{(1)}(0)) + O\left(\frac{1}{N^4}\right). \end{aligned}$$

The integral can be calculated by hand. It has the value

$$\int_0^\pi g(x) dx = -\ln(2)$$

so that

$$Q_2(N) = -\frac{1}{\pi} \ln(2) + \frac{\pi}{12N^2} + O\left(\frac{1}{N^4}\right). \quad (70)$$

Asymptotic Expansion of $Q_3^r(N)$ as $N \rightarrow \infty$: We defined $Q_3^r(N)$ as

$$Q_3^r(N) = \frac{4}{N} \sum_{m=1}^{\lfloor \frac{N-1}{2} \rfloor} \frac{\alpha_m^{rN}(1) [1 - \alpha_m^N(1)]^{-1}}{\sin(\frac{\pi}{N}m) [1 + \sin^2(\frac{\pi}{N}m)]^{\frac{1}{2}}},$$

r being a positive scalar. For $r = 1$, if N is held odd, since $N - m$ term equals m term, one can recognize that $Q_3^r(N) = Q_3(N)$. If N is even, the $\lfloor \frac{N-1}{2} \rfloor + 1$ term would have to be added separately to the sum up-bounded by $\lfloor \frac{N-1}{2} \rfloor$. In fact, as discussed in the following, this term can almost be neglected.

Studying $Q_3^r(N)$, note that the terms corresponding to values of m close to the lower bound, i.e., $m = 1$, contributes more significantly than the ones corresponding to values of m close to the upper bound, i.e., $m = \lfloor \frac{N-1}{2} \rfloor$. Indeed, if m is held close to $\lfloor \frac{N-1}{2} \rfloor$ and N is very large, then $\alpha_m(1)$ remains lower than 1, so $\alpha_m^N(1)$ vanishes exponentially to 0 as $N \rightarrow \infty$ while the other terms of the summand of $Q_3^r(N)$ go to a constant. Whereas, when m is held close to 1, $\alpha_m(1)$ goes to 1 as $N \rightarrow \infty$ and the summand of $Q_3^r(N)$ diverges.

In order to approximate $Q_3^r(N)$ when N is large, we use a method described in [21]. It consists of breaking the sum into two disjoint ranges \mathcal{D}_N and \mathcal{T}_N to be examined separately. The summation over \mathcal{D}_N -the smallest m here- is the ‘‘dominant’’ part, in the sense that it includes enough terms to determine the significant digits of the sum when N is large. The summation over the other range \mathcal{T}_N is the ‘‘tail’’ end, which contributes little to the overall total. Note that if N is even, the $\lfloor \frac{N-1}{2} \rfloor + 1$ term that would have to be added separately to the sum up-bounded by $\lfloor \frac{N-1}{2} \rfloor$ pertains to the ‘‘tail’’ and it is understood how it can be neglected.

Thus, if we separate out the dominant and the tail ranges for $Q_3^r(N)$, one has

$$Q_3^r(N) = \sum_{m \in \mathcal{D}_N} a_m(N) + \sum_{m \in \mathcal{T}_N} a_m(N), \quad (71)$$

where $a_m(N)$ is defined as

$$a_m(N) = \frac{4}{N} \times \frac{\alpha_m^{rN}(1) [1 - \alpha_m^N(1)]^{-1}}{\sin(\frac{\pi}{N}m) [1 + \sin^2(\frac{\pi}{N}m)]^{\frac{1}{2}}}.$$

As long as m is held in the dominant range, fraction $\frac{\pi}{N}m$ goes to zero as $N \rightarrow \infty$. Therefore, $a_m(N)$ can be developed according to the following asymptotic expansion as $N \rightarrow \infty$

$$a_m(N) = b_m(N) + O(c_m(N)) \quad (72)$$

where

$$\begin{aligned} b_m(N) &= \frac{4e^{-2\pi mr}}{\pi m [1 - e^{-2\pi m}]} \\ &\quad + \frac{4\pi m [e^{-2\pi m} + 2\pi m - 1] e^{-2\pi mr}}{3N^2 [1 - e^{-2\pi m}]^2} \end{aligned} \quad (73)$$

and

$$c_m(N) = \frac{m^3 e^{-2\pi mr}}{N^4 [1 - e^{-2\pi m}]}.$$

This asymptotic expansion is valid as long as $m \in \mathcal{D}_N$. Therefore, it is allowed to take the summation of both sides of (72) over \mathcal{D}_N . We obtain

$$\begin{aligned} \sum_{m \in \mathcal{D}_N} a_m(N) &= \sum_{m \in \mathcal{D}_N} b_m(N) + \sum_{m \in \mathcal{D}_N} O(c_m(N)) \\ &= \sum_{m \in \mathcal{D}_N} b_m(N) + O\left(\sum_{m \in \mathcal{D}_N} |c_m(N)|\right). \end{aligned}$$

We have now to find a good bound on the sum $\sum_{m \in \mathcal{D}_N} |c_m(N)|$. Indeed, we have

$$\sum_{m \in \mathcal{D}_N} |c_m(N)| \leq \frac{1}{N^4} \sum_{m=1}^{\infty} \frac{m^3 e^{-2\pi mr}}{1 - e^{-2\pi m}}.$$

However, $\sum_{m=1}^{\infty} \frac{m^3 e^{-2\pi mr}}{1 - e^{-2\pi m}}$ converges, then we obtain

$$\sum_{m \in \mathcal{D}_N} |c_m(N)| = O\left(\frac{1}{N^4}\right),$$

leading to

$$\sum_{m \in \mathcal{D}_N} a_m(N) = \sum_{m \in \mathcal{D}_N} b_m(N) + O\left(\frac{1}{N^4}\right). \quad (74)$$

Therefore, (71) can be rewritten as

$$\begin{aligned} Q_3^r(N) &= \sum_{m \in \mathcal{D}_N} b_m(N) + \sum_{m \in \mathcal{T}_N} a_m(N) + O\left(\frac{1}{N^4}\right) \\ &= \sum_{m \in \mathcal{D}_N \cup \mathcal{T}_N} b_m(N) + \sum_{m \in \mathcal{T}_N} a_m(N) \\ &\quad - \sum_{m \in \mathcal{T}_N} b_m(N) + O\left(\frac{1}{N^4}\right). \end{aligned} \quad (75)$$

Now, we evaluate the tail range contributions. It suffices to find good bounds on $\sum_{m \in \mathcal{T}_N} a_m(N)$ and $\sum_{m \in \mathcal{T}_N} b_m(N)$.

As long as m is held in \mathcal{T}_N , $\frac{\pi}{N}m$ converges to $\frac{\pi}{2}$ as $N \rightarrow \infty$. So, $\alpha_m(1)$ goes to $3 - 2\sqrt{2} < 1$. Hence, $\alpha_m^N(1)$ decreases faster than any power of $\frac{1}{N}$ as $N \rightarrow \infty$. It can be then deduced that

$$a_m(N) = O\left(\frac{1}{N^4}\right).$$

Thus,

$$\sum_{m \in \mathcal{T}_N} a_m(N) = O\left(\frac{1}{N^4}\right).$$

Similarly, when $m \in \mathcal{T}_N$, we can show that

$$b_m(N) = O(e^{-\pi N}).$$

Since $e^{-\pi N}$ vanishes faster than any power of $\frac{1}{N}$, in particular faster than $\frac{1}{N^4}$, then we can write

$$\sum_{m \in \mathcal{T}_N} b_m(N) = O\left(\frac{1}{N^4}\right).$$

Thus, we obtain (75) in the form of

$$\begin{aligned} Q_3^r(N) &= \sum_{m \in \mathcal{D}_N \cup \mathcal{T}_N} b_m(N) + O\left(\frac{1}{N^4}\right) + O\left(\frac{1}{N^4}\right) + O\left(\frac{1}{N^4}\right) \\ &= \sum_{m=1}^{\lfloor \frac{N-1}{2} \rfloor} b_m(N) + O\left(\frac{1}{N^4}\right) \\ &= \frac{4}{\pi} U_{N,0}^{(r)} + \frac{4\pi}{3N^2} U_{N,1}^{(r)} + O\left(\frac{1}{N^4}\right), \quad \text{where} \\ U_{N,k}^{(r)} &= \sum_{m=1}^{\lfloor \frac{N-1}{2} \rfloor} \frac{e^{-2\pi mr}}{m [1 - e^{-2\pi m}]} \times \left[\frac{m^2 [e^{-2\pi m} + 2\pi m - 1]}{[1 - e^{-2\pi m}]} \right]^k. \end{aligned}$$

$U_{N,k}^{(r)}$ converge as $N \rightarrow \infty$ for $k = 0, 1$. $\ell_k^{(r)}$ being related limits, since the exponential function grows faster than any power of N , it can be written

$$U_{N,k}^{(r)} = \ell_k^{(r)} + O\left(\frac{1}{N^4}\right). \quad (76)$$

So, computing $\ell_k^{(r)}$ for $k = 0, 1$ and $r = 1, \frac{1}{2}$ one gets

$$\begin{aligned} \ell_0^{(1)} &= 0.001872682450, \quad \ell_1^{(1)} = 0.009987520718, \\ \ell_0^{(\frac{1}{2})} &= 0.0442562963296, \quad \ell_1^{(\frac{1}{2})} = 0.277125049773. \end{aligned} \quad (77)$$

Otherwise, $Q_3^r(N)$ has the following asymptotic expansion as $N \rightarrow \infty$

$$Q_3^r(N) = \frac{4}{\pi} \ell_0^{(r)} + \frac{4\pi}{3N^2} \ell_1^{(r)} + O\left(\frac{1}{N^4}\right). \quad (78)$$

REFERENCES

- [1] K. Holger and A. Willing, *Protocols and Architectures for Wireless Sensor Networks*. New York: Wiley, 2005.
- [2] M. Hempstead, N. Tripathi, P. Mauro, G.-Y. Wei, and D. Brooks, "An ultra low power system architecture for sensor network applications," in *Proc. 32nd Int. Symp. Comput. Arch.*, Jun. 2005, pp. 208–219.
- [3] P. Juang, H. Oki, Y. Wang, M. Martonozi, L.-S. Peh, and D. Rubenstein, "Energy-efficient computing for wildlife tracking: Design trade-offs and early experiences with zebraNet," in *Proc. 10th Int. Conf. Arch. Support Program. Lang. Oper. Syst.*, Oct. 2002, pp. 96–107.

- [4] R. Cardell-Oliver, K. Smettem, M. Kranz, and K. Mayer, "A reactive soil moisture sensor network: Design and field evaluation," *Int. J. Distributed Sensor Networks*, vol. 1, no. 2, pp. 149–162, Jun. 2005.
- [5] P. Sikka, P. Corke, P. Valencia, C. Crossman, D. Swain, and G. Bishop-Hurley, "Wireless ad hoc sensor and actuator networks on the farm," in *Proc. 5th Int. Conf. Inf. Process. Sensor Netw.*, Apr. 2006, pp. 492–499.
- [6] "Efficient and lightweight wireless sensor communication systems – Novel cross optimization," in *e-SENSE IST-4-027227-Integrated Project, Capturing Ambient Intelligence for Mobile Communications through Wireless Sensor Networks*, Dec. 2007.
- [7] P. Chen, B. O'Dea, and E. Callaway, "Energy efficient system design with optimum transmission range for wireless ad hoc networks," in *Proc. IEEE Int. Conf. Communications*, Apr. 2002, vol. 1, pp. 945–952.
- [8] S. Ergen and P. Varaiya, "On multi-hop routing for energy efficiency," *IEEE Commun. Lett.*, vol. 9, no. 10, pp. 880–881, Oct. 2005.
- [9] G. Xing, C. Lu, Y. Zhang, and Q. Huang, "Minimum power configuration in wireless sensor networks," in *Proc. 6th ACM Int. Symp. Mobile Ad Hoc Networking and Computing*, May 2005, pp. 390–401.
- [10] R. Shah and J. M. Rabaey, "Energy aware routing for low energy ad hoc sensor networks," in *Proc. IEEE Wireless Communications and Networking Conf.*, Mar. 2002, pp. 812–817, 1.
- [11] J.-H. Chang and L. Tassiulas, "Maximum lifetime routing in wireless sensor networks," *IEEE/ACM Trans. Networking*, vol. 12, no. 4, pp. 609–619, Apr. 2004.
- [12] Y. T. Hou, Y. Shi, and H. D. Sherali, "On lexicographic max-min node lifetime for wireless sensor networks," in *Proc. IEEE Int. Conf. Communications*, Jun. 2004, pp. 3790–3796.
- [13] S. D. Servetto and G. Barrenechea, "Constrained random walks on random graphs: Routing algorithms for large scale wireless sensor networks," in *Proc. 1st ACM Int. Workshop Wireless Sensor Netw. Applicat.*, New York, NY, 2002, pp. 12–21.
- [14] A. Vahdat and D. Becker, "Epidemic routing for partially connected ad hoc networks," Duke University, Tech. Rep. CS-200006, 2000.
- [15] Z. Haas, J. Halpern, and L. Li, "Gossip-based ad hoc routing," in *Proc. 21st Annu. Conf. Comput. Commun.*, Jun. 2002, pp. 1707–1716.
- [16] O. Dousse, "Asymptotic properties of wireless multi-hop network," Ph.D. dissertation, École Polytechnique Fédérale de Lausanne, Switzerland, 2005.
- [17] D. Braginsky and D. Estrin, "Rumor routing algorithm for sensor networks," in *Proc. 1st ACM Int. Workshop Wireless Sensor Netw. Applicat.*, New York, NY, 2002, pp. 22–31.
- [18] M. Zhong and K. Shen, "Random walk based node sampling in self-organizing networks," *Oper. Syst. Rev.*, vol. 40, no. 3, pp. 49–55, 2006.
- [19] J. Kleinberg, "The small-world phenomenon: An algorithmic perspective," Cornell, Ithaca, NY, Tech. Rep., 1999.
- [20] B. D. Hughes, *Random Walks and Random Environments*. Oxford, U.K.: Oxford Science, 1995, vol. 1.
- [21] R. Graham, D. Knuth, and O. Patashnik, *Concrete Mathematics: A Foundation of Computer Science*, 2nd ed. Reading, MA: Addison-Wesley, 1994.
- [22] E. Duarte-Melo and L. Mingyan, "Analysis of energy consumption and lifetime of heterogeneous wireless sensor networks," in *Proc. Global Telecommunication Conf.*, Nov. 2002, vol. 1, pp. 21–25.
- [23] L. Lima and J. Barros, "Random walks on sensor networks," in *Proc. 5th Int. Symp. Modelling and Optimization in Mobile, Ad Hoc, and Wireless Networks*, Apr. 2007.

Gwillerm Froc received the Ph.D. degree in physics in 1997 from the University of Paris XI, France.

He has been with Mitsubishi-Electric R&D Centre Europe since 2001. His current main scientific and engineering interests deal with the design and the modelling of wireless ad hoc networks with special focus on lightweight wireless sensor systems.

Issam Mabrouki received the Master's degree from École Centrale des Arts et Manufactures, Paris, France, in 2002, and the M.S degree in computer science from the École Nationale Supérieure des Télécommunications, Paris, France, in 2004. He is currently pursuing the Ph.D. degree at Telecom Bretagne, France, in collaboration with Mitsubishi-Electric R&D Centre Europe. His current interests include stochastic process modeling in computer and telecommunication systems.

Xavier Lagrange received the Engineering Degree from École Centrale des Arts et Manufactures, Paris, France, in 1984 and the Ph.D. degree from ENST in 1998.

He is currently a Professor at Telecom Bretagne (Rennes), France, in the Multimedia, Security and Network Department. His current research interests include resource allocation and teletraffic analysis of wireless and ad hoc network works.